

Non-linear optical response of non-interacting systems with spectral methods

S. M. João

*Centro de Física das Universidades do Minho e Porto and
Departamento de Física e Astronomia, Faculdade de Ciências,
Universidade do Porto, 4169-007 Porto, Portugal*

J. M. V. P. Lopes

*Centro de Física das Universidades do Minho e Porto
Departamento de Engenharia Física, Faculdade de Engenharia and
Departamento de Física e Astronomia, Faculdade de Ciências,
Universidade do Porto, 4169-007 Porto, Portugal*

A perturbation expansion is developed using the Keldysh formalism to obtain the nonlinear optical conductivity of non-interacting systems with special focus on Tight-Binding models. This basis-independent approach provides the objects required by numerical spectral methods, allowing for a straightforward numerical implementation of the optical conductivity in any order of the perturbation expansion. With this formalism, it is possible to introduce disorder and magnetic fields in numerical Tight-Binding computations of nonlinear optical responses.

I. INTRODUCTION

Since the advent of the laser in 1960, the field of non-linear optics has received considerable interest. The following year marked the beginning of a systematic study of this field, as in 1961 P. Franken was able to demonstrate second harmonic generation (SHG) [6] experimentally. This opened the gateway to a whole new plethora of phenomena, such as optical rectification (1962) [2] and higher harmonic generation (1967) [14]. For the effects to be noticeable, this external field had to be comparable to the electric field inside the crystal, which is typically of the order of 10^8 V/m. Shining a laser on a sample also provides a way to probe the material's transport properties. The transport properties in crystals have been studied extensively throughout the last 30 years [20] and have recently received considerable interest due to the strong non-linear properties of layered materials such as graphene [3, 8, 13].

Many approaches to obtain the non-linear response of a crystalline system subject to an external field have been reported. Among those, we may find generalizations of Kubo's formula for higher orders [1] and perturbation expansions for the density matrix in both the length gauge and the velocity gauge [20, 21]. In this work, we used the Keldysh formalism [10] to develop a general perturbation procedure to deal with non-interacting fermion systems at finite temperature coupled to a time-dependent external field. Through careful categorization of all these contributions, we provide a systematic procedure to find the objects needed to calculate the conductivity at any order. These objects are expressed with no reference to a specific basis. Most of the approaches mentioned thus far assume translation invariance to do the calculations in momentum basis. This approach does not rely on translation invariance and thus allows us to easily include structural disorder and magnetic fields in our numerical simulations.

The critical point here is that the mathematical objects provided by our perturbation expansion are precisely the ones required by the numerical spectral methods we use. This fact, combined with the diagrammatic approach developed by us, provides a straightforward way to implement the numerical calculation of the nonlinear optical conductivity for a wide range of materials. These calculations are implemented in an open-source project developed by ourselves [12] and the results are shown in Section V.

This paper is structured as follows. In Section II, we introduce the Keldysh formalism to show how the current will be calculated and define the fundamental mathematical objects of our calculations. Section III applies the perturbation procedure to a Tight-Binding model. The electromagnetic field is added through the Peierls Substitution. Then, a diagrammatic procedure is developed in order to deal with the large number of non-trivial contributions to the conductivity in each order. Section IV explains how to use a Chebyshev expansion of the operators in the previous expression in order to be used with spectral methods. This provides the full formula that may be directly implemented numerically. Finally, in Section V we apply the formalism developed in the previous sections to three different systems: Graphene; hexagonal Boron Nitride (h-BN); and a slight variation of h-BN where one of the sublattices is displaced relative to the other.

II. KELDYSH FORMALISM

The Keldysh formalism [5, 11, 19] is a general perturbation scheme describing the quantum mechanical time evolution of non-equilibrium interacting systems at finite temperature. It provides a concise diagrammatic representation of the average values of quantum operators.

This formalism does not rely on any particular basis, which is a critical feature for this paper. The mathematical objects obtained in our expansion are in the form required by numerical spectral methods, providing a straightforward formula for the numerical calculation of nonlinear optical response functions. In this section we will introduce the definitions of the objects used throughout the paper and show how to expand the Green's functions for fermions [10] with this formalism.

A. Definitions

1. Green's functions

To use the Keldysh formalism for fermions, we need the definitions of the time-ordered, lesser, greater and anti-time-ordered Green's functions. Respectively,

$$iG_{ab}^T(t, t') = \langle T [c_a(t) c_b^\dagger(t')] \rangle \quad (1)$$

$$iG_{ab}^<(t, t') = -\langle c_b^\dagger(t') c_a(t) \rangle \quad (2)$$

$$iG_{ab}^>(t, t') = \langle c_a(t) c_b^\dagger(t') \rangle \quad (3)$$

$$iG_{ab}^{\tilde{T}}(t, t') = \langle \tilde{T} [c_a(t) c_b^\dagger(t')] \rangle. \quad (4)$$

All the creation and annihilation operators are in the Heisenberg picture and the labels a and b denote states belonging to a complete single-particle basis. T is the time-ordering operator and \tilde{T} the anti-time-ordering operator. The average $\langle \dots \rangle$ stands for $\text{Tr}[\rho(t_0) \dots] / \text{Tr}[\rho(t_0)]$ in the grand canonical ensemble, ρ is the density matrix and t_0 denotes the time at which the external perturbation has been switched on. These are the building blocks of the Keldysh formalism. The advanced and retarded Green's functions are a simple combination of the previous objects:

$$G^R = G^T - G^< \quad (5)$$

$$G^A = -G^{\tilde{T}} + G^<. \quad (6)$$

The non-perturbed versions of these Green's functions are denoted by a lowercase g .

2. Expected value of an operator

The expected value of the current $\mathbf{J}(t)$ (or any one-particle operator) may be evaluated with resort to these Green's functions by tracing over its product with the perturbed lesser Green's function:

$$\mathbf{J}(t) = \langle \hat{\mathbf{J}}(t) \rangle = -\text{Tr} [\hat{\mathbf{J}}(t) iG^<(t, t)]. \quad (7)$$

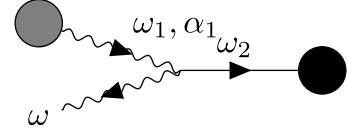


Figure 1: Diagrammatic representation of the expected value of the current operator in Fourier space. The horizontal straight line ending in a circle is the lesser Green's function and the wavy line beginning in a circle represents the current operator.

The Fourier transform [23] of $\mathbf{J}(t)$ is shown diagrammatically in Figure 1. The circles stand for the full, perturbed operators in the presence of an external field.

3. Conductivity

We use the same definition for the nonlinear optical conductivity as in [16, 21]:

$$J^\alpha(\omega) = \sigma^{\alpha\beta}(\omega) E^\beta(\omega) + \int \frac{d\omega_1}{2\pi} \int \frac{d\omega_2}{2\pi} \times \quad (8)$$

$$\sigma^{\alpha\beta\gamma}(\omega_1, \omega_2) E^\beta(\omega_1) E^\gamma(\omega_2) 2\pi\delta(\omega_1 + \omega_2 - \omega) + \dots$$

The next section is devoted to finding the perturbation expansion of $G^<$. In this paper we are dealing with Tight-Binding models, in which case the current operator will itself be a power series of the external field.

B. Non-interacting electronic systems

Our system is described by the many-particle time-dependent Hamiltonian

$$\mathcal{H}(t) = \mathcal{H}_0 + \mathcal{H}_{\text{ext}}(t). \quad (9)$$

where \mathcal{H}_0 is an Hamiltonian that we can solve exactly and $\mathcal{H}_{\text{ext}}(t)$ is the time-dependent external perturbation. Here we restrict ourselves to non-interacting Hamiltonians since we're dealing with non-interacting electrons. These operators are expressed in terms of their single-particle counterparts as

$$\mathcal{H}_{\text{ext}}(t) = \sum_{ab} [\mathcal{H}_{\text{ext}}(t)]_{ab} c_a^\dagger(t) c_b(t) \quad (10)$$

$$\mathcal{H}_0 = \sum_{ab} [H_0]_{ab} c_a^\dagger(t) c_b(t). \quad (11)$$

The expansion of the perturbed lesser Green's function $G^<$ will be expressed in terms of the unperturbed Green's functions $g^>$, $g^<$, g^R and g^A in Fourier space:

$$i\tilde{g}^<(\omega) = -2\pi f(\hbar\omega) \delta(\omega - H_0/\hbar) \quad (12)$$

$$i\tilde{g}^>(\omega) = 2\pi [1 - f(\hbar\omega)] \delta(\omega - H_0/\hbar) \quad (13)$$

$$i\tilde{g}^R(\omega) = \frac{i}{\omega - H_0/\hbar + i0^+} \quad (14)$$

$$i\tilde{g}^A(\omega) = \frac{i}{\omega - H_0/\hbar - i0^+}, \quad (15)$$

where $f(\epsilon) = (1 + e^{\beta(\epsilon - \mu)})^{-1}$ is the Fermi-Dirac distribution, β is the inverse temperature and μ is the chemical potential. The Keldysh formalism and Langreth's rules provide the perturbation expansion of $G^<$ [10]. Defining $V(t) = (i\hbar)^{-1} H_{\text{ext}}(t)$, the zeroth-order term in the expansion is

$$i\tilde{G}^{<(0)}(\omega) = \int d\omega_1 i\tilde{g}^<(\omega_1) \delta(\omega) \quad (16)$$

and the first-order one is

$$\begin{aligned} i\tilde{G}^{<(1)}(\omega) = & \int \frac{d^3\omega_{123}}{(2\pi)^3} (2\pi)^2 \delta(\omega_1 - \omega_2 - \omega_3) \\ & \times \delta(\omega + \omega_3 - \omega_1) \left[i\tilde{g}^R(\omega_1) \tilde{V}(\omega_2) i\tilde{g}^<(\omega_3) + \right. \\ & \left. + i\tilde{g}^<(\omega_1) \tilde{V}(\omega_2) i\tilde{g}^A(\omega_3) \right]. \end{aligned} \quad (17)$$

$\int d^n\omega_{1\dots n}$ is a shorthand for $\int \dots \int d\omega_1 \dots d\omega_n$. The second-order term is

$$\begin{aligned} i\tilde{G}^{<(2)}(\omega) = & \int \frac{d^5\omega_{1\dots 5}}{(2\pi)^5} (2\pi)^3 \delta(\omega_5 + \omega - \omega_1) \times \\ & \delta(\omega_1 - \omega_2 - \omega_3) \delta(\omega_3 - \omega_4 - \omega_5) \times \\ & \left[i\tilde{g}^R(\omega_1) \tilde{V}(\omega_2) i\tilde{g}^R(\omega_3) \tilde{V}(\omega_4) i\tilde{g}^<(\omega_5) \right. \\ & + i\tilde{g}^R(\omega_1) \tilde{V}(\omega_2) i\tilde{g}^<(\omega_3) \tilde{V}(\omega_4) i\tilde{g}^A(\omega_5) \\ & \left. + i\tilde{g}^<(\omega_1) \tilde{V}(\omega_2) i\tilde{g}^A(\omega_3) \tilde{V}(\omega_4) i\tilde{g}^A(\omega_5) \right]. \end{aligned} \quad (18)$$

Diagrammatically, the expansion of $iG^<(\omega)$ is represented by Figure 2. Each wavy line ending in a circle represents an external perturbation \tilde{V} . There are three different types of Green's functions that may appear in these expansions, with a certain regularity: a lesser Green's function $\tilde{g}^<$ is always present; to its left there can only be retarded functions and to its right, advanced functions. Diagrammatically, $\tilde{g}^<$ is represented by a dashed line while the straight lines after it (clockwise) represent retarded Green's functions and the ones before, advanced Green's functions. In each intersection, the corresponding external perturbation \tilde{V} is inserted. An exception is made for the intersection with the line representing ω , as it still needs to be contracted.

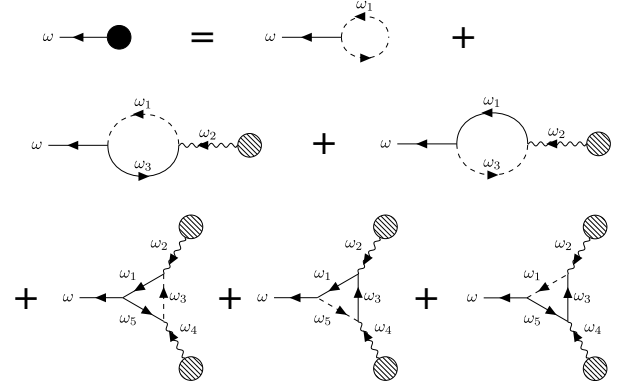


Figure 2: Diagrammatic representation of the lesser Green's function.

If the external perturbation were a simple external field $\mathbf{E}(t)$, then the coupling would be $H_{\text{ext}}(t) = e\mathbf{E}(t) \cdot \mathbf{r}$ and the previous expressions coupled with eq. (7) would suffice. Now we will turn to Tight-Binding Hamiltonians, for which the external coupling is actually an infinite series of operators due to the way the electromagnetic field is introduced. This affects not only the V operators but also the expression for the current operator.

III. TIGHT BINDING HAMILTONIAN WITH EXTERNAL ELECTRIC FIELD

Tight-Binding models provide a simple framework with which to calculate transport quantities. It can be used to express structural disorder in the system, whilst Peierls' substitution [17] imbues the system with an electromagnetic field. Despite the simplicity of this procedure, the addition of an electromagnetic field through a phase factor yields an infinite series of terms in H_{ext} . In this section, we obtain the expression for H_{ext} and show how the expansions of the previous sections may be used to obtain the nonlinear optical conductivity.

A. Series expansion

Let's consider the following Tight-Binding Hamiltonian:

$$\mathcal{H}_0 = \sum_{\mathbf{R}_i, \mathbf{R}_j} \sum_{\sigma_1, \sigma_2} t_{\sigma_1 \sigma_2}(\mathbf{R}_i, \mathbf{R}_j) c_{\sigma_1}^\dagger(\mathbf{R}_i) c_{\sigma_2}(\mathbf{R}_j). \quad (19)$$

The \mathbf{R}_i represent the lattice sites and the σ_i the other degrees of freedom unrelated to the position, such as the orbitals and spin. The electromagnetic field is introduced through Peierls' substitution:

$$t_{\sigma_1 \sigma_2}(\mathbf{R}_i, \mathbf{R}_j) \rightarrow e^{\frac{-ie}{\hbar} \int_{\mathbf{R}_j}^{\mathbf{R}_i} \mathbf{A}(\mathbf{r}', t) \cdot d\mathbf{r}'} t_{\sigma_1 \sigma_2}(\mathbf{R}_i, \mathbf{R}_j) \quad (20)$$

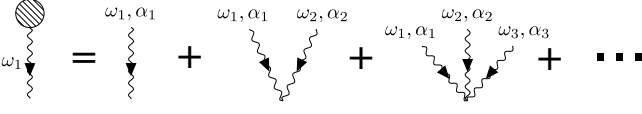


Figure 3: Diagrammatic representation of the external perturbation.

To introduce both a static magnetic field and a uniform electric field, we use the following vector potential:

$$\mathbf{A}(\mathbf{r}, t) = \mathbf{A}_1(\mathbf{r}) + \mathbf{A}_2(t). \quad (21)$$

The electric and magnetic fields are obtained from $\mathbf{E}(t) = -\partial_t \mathbf{A}_2(t)$ and $\mathbf{B}(\mathbf{r}) = \nabla \times \mathbf{A}_1(\mathbf{r})$. The introduction of the magnetic field only changes the $t_{\sigma_1 \sigma_2}(\mathbf{R}_i, \mathbf{R}_j)$ without introducing a time-dependency. Therefore, we may assume that a magnetic field is always present without any loss of generality for the following discussion while keeping in mind that its introduction broke translation invariance. Since the magnetic field only affects the hopping parameters, from now on the term in the vector potential that provides the electric field will be denoted by $\mathbf{A}(t)$. The external perturbation is obtained by expanding the exponential in eq. 20 and identifying the original Hamiltonian.

1. Expansion of the external perturbation

Expanding the exponential in eq. 20 yields an infinite series of operators for the full Hamiltonian:

$$H_{\mathbf{A}}(t) = H_0 + H_{\text{ext}}(t) \quad (22)$$

from which we identify, after a Fourier transform,

$$\tilde{V}(\omega) = \frac{e}{i\hbar} h^\alpha \tilde{A}^\alpha(\omega) + \frac{e^2}{i\hbar} \frac{h^{\alpha\beta}}{2!} \int \frac{d\omega'}{2\pi} \int \frac{d\omega''}{2\pi} \times (23)$$

$$\tilde{A}^\alpha(\omega') \tilde{A}^\beta(\omega'') 2\pi \delta(\omega' + \omega'' - \omega) + \dots$$

Repeated spatial indices are understood to be summed over. We have defined

$$\hat{h}^{\alpha_1 \dots \alpha_n} = \frac{1}{(i\hbar)^n} [\hat{r}^{\alpha_1}, [\dots [\hat{r}^{\alpha_n}, H_0]]] \quad (24)$$

where \hat{r} is the position operator. In first order, \hat{h}^α is just the single-particle velocity operator. In Figure 3 we see how the diagrammatic representation of the external perturbation unfolds into an infinite series of external fields. The dashed line ending in a cross represents $\tilde{\mathbf{A}}$ and the number of external fields connected to the same point represents the number of commutators in eq. 24.

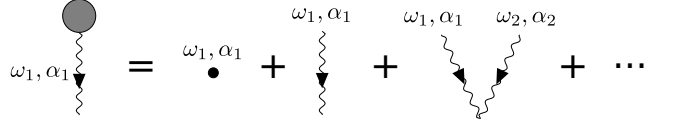


Figure 4: Diagrammatic representation of the current operator. The single small circle is to be understood as a Dirac delta.

2. Expansion of the current

The current operator is calculated directly from the Hamiltonian, using $\hat{J}^\alpha = -\Omega^{-1} \partial H / \partial A^\alpha$ (Ω is the volume of the sample), which also follows a series expansion due to the presence of an infinite number of $\mathbf{A}(t)$ in H_{ext} :

$$\hat{J}^\alpha(t) = -\frac{e}{\Omega} \left(\hat{h}^\alpha + e \hat{h}^{\alpha\beta} A^\beta(t) + \frac{e^2}{2!} \hat{h}^{\alpha\beta\gamma} A^\beta(t) A^\gamma(t) + \dots \right). \quad (25)$$

Figure 4 depicts the diagrammatic representation of this operator in Fourier space. Note that the line representing ω is always present and is pointing outwards.

The complexity of this expansion becomes clear. In eq. 7, both the current operator and the Green's functions follow a perturbation expansion. Furthermore, each interaction operator in every one of the terms in the Green's function expansion also follows a similar expansion. We now have all the objects needed for the perturbative expansion of the conductivity.

B. Perturbative expansion of the conductivity

In the previous sections we laid out the expressions for each individual operator in our expansion and represented their corresponding diagrammatic depictions. In this subsection, we put together all the elements of the previous sections to provide the full diagrammatic representation of the first and second-order conductivities. This expansion closely resembles that of [15] but has several differences due to the usage of these specific Green's functions. The only thing left to do is to replace the perturbed objects in the diagrammatic representation of the expected value of the current operator by their expansions. It is straightforward to see how the diagrams fit together in Figure 5, which shows all the contributing diagrams up to second order.

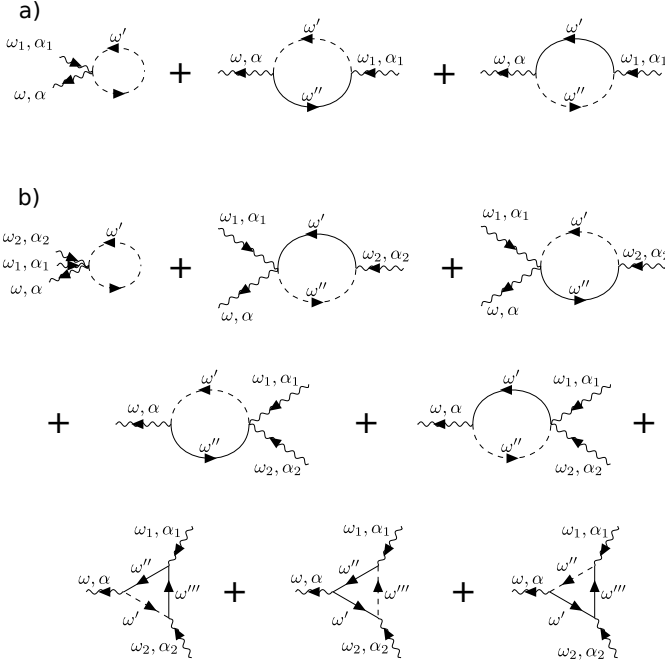


Figure 5: Expansion of the expected value of the conductivity in (a) first and (b) second order.

Obtaining the conductivity from the current is a matter of expressing the frequencies ω' , ω'' and ω''' in terms of ω_1 , ω_2 and ω and using $\mathbf{E}(\omega) = i\omega\mathbf{A}(\omega)$. The Dirac

delta in eq. 8 simply means that ω is to be replaced by the sum of external frequencies entering the diagram. Thus, the n -th order conductivity may be found using the following rules:

1. Draw all the diagrams with n dashed lines coming in the diagram, one going out and one wavy interconnecting line. Integrate over the internal frequencies and ignore the conservation of momentum in the vertex containing ω , as that is already taken into account by the Dirac delta in the definition of the conductivity.
2. Reading clockwise starting from the vertex containing ω , insert, by order, a generalized velocity operator $\hat{h}^{\alpha_1 \dots \alpha_k}$ at each vertex and a Green's function at each edge. Each α_i is the label of a frequency line connecting to the vertex. If the edge is wavy, the Green's function is $ig^<$. All the edges before that correspond to ig^R and the ones after it to ig^A . Trace over the resulting operator.
3. Multiply by $\Omega^{-1}e^{n+1} \prod_{k=1}^n (i\omega_k)^{-1} (i\hbar)^{1-N}$, where n is the number of dashed lines and N is the number of interconnecting lines. For each vertex, divide by the factorial of the number of outgoing lines.

Following these rules and replacing $ig^<$ by eq. 12, the first-order conductivity is found:

$$\sigma^{\alpha\beta}(\omega) = \frac{ie^2}{\Omega\omega} \int_{-\infty}^{\infty} d\epsilon f(\epsilon) \text{Tr} \left[\hat{h}^{\alpha\beta} \delta(\epsilon - H_0) + \frac{1}{\hbar} \hat{h}^{\alpha} g^R(\epsilon/\hbar + \omega) \hat{h}^{\beta} \delta(\epsilon - H_0) + \frac{1}{\hbar} \hat{h}^{\alpha} \delta(\epsilon - H_0) \hat{h}^{\beta} g^A(\epsilon/\hbar - \omega) \right]. \quad (26)$$

Similarly, for the second-order conductivity:

$$\begin{aligned} \sigma^{\alpha\beta\gamma}(\omega_1, \omega_2) = & \frac{1}{\Omega} \frac{e^3}{\omega_1 \omega_2} \int_{-\infty}^{\infty} d\epsilon f(\epsilon) \text{Tr} \left[\frac{1}{2} \hat{h}^{\alpha\beta\gamma} \delta(\epsilon - H) + \frac{1}{\hbar} \hat{h}^{\alpha\beta} g^R(\epsilon/\hbar + \omega_2) \hat{h}^{\gamma} \delta(\epsilon - H) \right. \\ & + \frac{1}{\hbar} \hat{h}^{\alpha\beta} \delta(\epsilon - H) \hat{h}^{\gamma} g^A(\epsilon/\hbar - \omega_2) + \frac{1}{2\hbar} \hat{h}^{\alpha} g^R(\epsilon/\hbar + \omega_1 + \omega_2) \hat{h}^{\beta\gamma} \delta(\epsilon - H) + \frac{1}{2\hbar} \hat{h}^{\alpha} \delta(\epsilon - H) \hat{h}^{\beta\gamma} g^A(\epsilon/\hbar - \omega_1 - \omega_2) \\ & + \frac{1}{\hbar^2} \hat{h}^{\alpha} g^R(\epsilon/\hbar + \omega_1 + \omega_2) \hat{h}^{\beta} g^R(\epsilon/\hbar + \omega_2) \hat{h}^{\gamma} \delta(\epsilon - H) + \frac{1}{\hbar^2} \hat{h}^{\alpha} g^R(\epsilon/\hbar + \omega_1) \hat{h}^{\beta} \delta(\epsilon - H) \hat{h}^{\gamma} g^A(\epsilon/\hbar - \omega_2) \\ & \left. + \frac{1}{\hbar^2} \hat{h}^{\alpha} \delta(\epsilon - H) \hat{h}^{\beta} g^A(\epsilon/\hbar - \omega_1) \hat{h}^{\gamma} g^A(\epsilon/\hbar - \omega_1 - \omega_2) \right]. \end{aligned} \quad (27)$$

The n -th order conductivity will have $2^{n-1}(n+2)$ diagrams. We will not obtain any higher-order expansion because those traces would require tremendous computa-

tional power, as will become evident in the next section.

IV. SPECTRAL METHODS

From the previous section, it becomes clear that the only objects needed to calculate the conductivity up to any order are the retarded and advanced Green's functions, Dirac deltas and the generalized velocity operators. In order to implement these calculations numerically, we use a stochastic evaluation of traces coupled with an expansion of those objects in Chebyshev polynomials of the Hamiltonian. Expressing the functions of the Hamiltonian as a series of Chebyshev polynomials allows for a very efficient and numerically stable method of calculating these traces [22]. The only functions of the Hamiltonian present in the expansion are Dirac deltas and Green's functions. Their highly singular nature means that convergence to the exact function is very difficult. Some methods like KPM add a weight function [7, 18] to each term in the expansion, effectively damping the oscillations. Although the oscillation disappear, it is not possible to converge to a Dirac delta, as adding more terms to the expansion always changes the result, bringing it closer to an "exact" Dirac delta. This presents some difficulties when assessing the convergence of the calculation. Instead, we use an exact decomposition of the broadened Green's function[4] with $0^+ \rightarrow \lambda$. A finite λ removes the singular nature of the Green's functions, allowing for the convergence to the exact function. The term \hbar/λ may also be interpreted as a typical relaxation time.

A. Expansion in Chebyshev polynomials

The Chebyshev polynomials are a set of orthogonal polynomials defined in the range $[-1, 1]$ through

$$T_n(x) = \cos(n \arccos(x)). \quad (28)$$

They satisfy a recursion relation

$$T_{n+1}(x) = 2xT_n(x) - T_{n-1}(x) \quad (29)$$

and the following orthogonality relation

$$\int_{-1}^1 T_n(x) T_m(x) \frac{dx}{\sqrt{1-x^2}}. \quad (30)$$

These polynomials may be used to expand functions of the Hamiltonian provided its spectrum has been scaled to fit in the range $[-1, 1]$. The only functions of the Hamiltonian appearing in the expansion are Dirac deltas and Green's functions, which have the following expansions in terms of Chebyshev polynomials:

$$\delta(\epsilon - H_0) = \sum_{n=0}^{\infty} \Delta_n(\epsilon) \frac{T_n(H_0)}{1 + \delta_{n0}} \quad (31)$$

$$g^{\sigma,\lambda}(\epsilon, H_0) = \frac{\hbar}{\epsilon - H_0 + i\sigma\lambda} = \hbar \sum_{n=0}^{\infty} g_n^{\sigma,\lambda}(\epsilon) \frac{T_n(H_0)}{1 + \delta_{n0}} \quad (32)$$

where

$$\Delta_n(\epsilon) = \frac{2T_n(\epsilon)}{\pi\sqrt{1-\epsilon^2}} \quad (33)$$

and

$$g_n^{\sigma,\lambda}(\epsilon) = -2\sigma i \frac{e^{-ni\sigma \arccos(\epsilon+i\sigma\lambda)}}{\sqrt{1-(\epsilon+i\sigma\lambda)^2}}. \quad (34)$$

The function $g^{\sigma,\lambda}$ encompasses both retarded and advanced Green's functions in the limit $\lambda \rightarrow 0^+$: $g^{+,0^+}$ is the retarded Green's function and $g^{-,0^+}$ the advanced one. The operator part has been completely separated from its frequency arguments. All the Dirac deltas and Green's functions may therefore be separated into a polynomial of H_0 and a coefficient which encapsulates the frequency and energy parameters. The trace in the conductivity now becomes a trace over a product of polynomials and \hat{h} operators, which can be encapsulated in a new object, the Γ matrix:

$$\Gamma_{n_1 \dots n_m}^{\alpha_1, \dots, \alpha_m} = \frac{\text{Tr}}{N} \left[\tilde{h}^{\alpha_1} \frac{T_{n_1}(H_0)}{1 + \delta_{n_1 0}} \dots \tilde{h}^{\alpha_m} \frac{T_{n_m}(H_0)}{1 + \delta_{n_m 0}} \right]. \quad (35)$$

The upper indices in bold stand for any number of indices: $\alpha_1 = \alpha_1^1 \alpha_1^2 \dots \alpha_1^{N_1}$. Here we have used $\tilde{h}^{\alpha_1} = (i\hbar)^{N_1} \hat{h}^{\alpha_1}$ rather than \hat{h} to avoid using complex numbers when the Hamiltonian matrix is purely real in our numerical simulations. It's very important to keep in mind that these new operators are no longer hermitian. The commas in Γ separate the various \tilde{h} operators. N is the number of unit cells in the sample being studied and ensures that Γ is an intensive quantity. Some examples:

$$\Gamma_{nm}^{\alpha, \beta\gamma} = \frac{\text{Tr}}{N} \left[\tilde{h}^{\alpha} \frac{T_n(H_0)}{1 + \delta_{n0}} \tilde{h}^{\beta\gamma} \frac{T_m(H_0)}{1 + \delta_{m0}} \right] \quad (36)$$

$$\Gamma_n^{\alpha\beta} = \frac{\text{Tr}}{N} \left[\tilde{h}^{\alpha\beta} \frac{T_n(H_0)}{1 + \delta_{n0}} \right] \quad (37)$$

$$\Gamma_{nmp}^{\alpha, \beta, \gamma} = \frac{\text{Tr}}{N} \left[\tilde{h}^{\alpha} \frac{T_n(H_0)}{1 + \delta_{n0}} \tilde{h}^{\beta} \frac{T_m(H_0)}{1 + \delta_{m0}} \tilde{h}^{\gamma} \frac{T_p(H_0)}{1 + \delta_{p0}} \right] \quad (38)$$

The Γ matrix only depends on the physical system itself as it is merely a function of the Hamiltonian and the

\tilde{h} operators. The coefficients of the Chebyshev expansion may similarly be aggregated into a matrix, which we denote by Λ . Some examples:

$$\Lambda_n = \int_{-\infty}^{\infty} d\epsilon f(\epsilon) \Delta_n(\epsilon) \quad (39)$$

$$\Lambda_{nm}(\omega) = \hbar \int_{-\infty}^{\infty} d\epsilon f(\epsilon) [g_n^R(\epsilon/\hbar + \omega) \Delta_m(\epsilon) + \Delta_n(\epsilon) g_m^A(\epsilon/\hbar - \omega)] \quad (40)$$

and

$$\begin{aligned} \Lambda_{nmp}(\omega_1, \omega_2) = & \quad (41) \\ & \hbar^2 \int_{-\infty}^{\infty} d\epsilon f(\epsilon) [g_n^R(\epsilon/\hbar + \omega_1 + \omega_2) g_m^R(\epsilon/\hbar + \omega_2) \Delta_p(\epsilon) \\ & + g_n^R(\epsilon/\hbar + \omega_1) \Delta_m(\epsilon) g_p^A(\epsilon/\hbar - \omega_2) \\ & + \Delta_n(\epsilon) g_m^A(\epsilon/\hbar - \omega_1) g_p^A(\epsilon/\hbar - \omega_1 - \omega_2)] \end{aligned}$$

In terms of these new objects, the conductivities become

$$\sigma^{\alpha\beta}(\omega) = \frac{-ie^2}{\Omega_c \hbar^2 \omega} \left[\sum_n \Gamma_n^{\alpha\beta} \Lambda_n + \sum_{nm} \Lambda_{nm}(\omega) \Gamma_{nm}^{\alpha,\beta} \right] \quad (42)$$

in first order and

$$\begin{aligned} \sigma^{\alpha\beta\gamma}(\omega_1, \omega_2) = & \frac{ie^3}{\Omega_c \omega_1 \omega_2 \hbar^3} \left[\frac{1}{2} \sum_n \Lambda_n \Gamma_n^{\alpha\beta\gamma} \right. \\ & + \sum_{nm} \Lambda_{nm}(\omega_2) \Gamma_{nm}^{\alpha\beta,\gamma} + \frac{1}{2} \sum_{nm} \Lambda_{nm}(\omega_1 + \omega_2) \Gamma_{nm}^{\alpha,\beta\gamma} \\ & \left. + \sum_{nmp} \Lambda_{nmp}(\omega_1, \omega_2) \Gamma_{nmp}^{\alpha,\beta,\gamma} \right] \quad (43) \end{aligned}$$

in second order. Ω_c is the volume of the unit cell.

B. Considerations on the numerical storage of Γ

Naturally, one cannot expect to sum the entire Chebyshev series, so it has to be truncated at some point N_{\max} . Each of the entries in a Γ matrix represents a complex number. Numerically, this is represented as two double-precision floating-point numbers, each taking up 8 bytes of storage. The amount of storage needed to store a Γ matrix of rank n is $16N_{\max}^n$. The number of Chebyshev polynomials needed to obtain a decent resolution depends heavily on the problem at hand, but a typical number may be $N_{\max} = 1024$. A rank 1 Γ matrix would take up 16 Kb of storage, a rank 2 matrix 16 Mb and a rank 3 matrix 16 Gb. Rank 3 matrices appear in the

second order conductivity. The third order conductivity would require a rank 4 matrix and as such, 16 Tb of storage. Numbers like these make it unfeasible to go beyond second order.

V. NUMERICAL RESULTS

As a proof of concept, we apply eq. 42 to several systems, starting with graphene. The existence of an inversion centre means that all the second order terms are zero. Hexagonal Boron Nitride (h-BN) has the same honeycomb lattice but each sublattice is made of a different atom, breaking this symmetry. Despite this fact, it can be proven[24] that the Γ matrices with three indices are zero, facilitating the computation of the second-order conductivity. In order to study the rank 3 Γ matrices, we have to further break the symmetry. Changing the relative position of the sublattices in h-BN is enough. The resulting lattice configuration resembles that of phosphorene, although the hopping parameters used are different. These three systems provide us with enough variety to study all the terms of the second order response.

A. Honeycomb lattice

Let a be the distance between consecutive atoms in the honeycomb lattice. Then, the primitive vectors between unit cells are (see Fig. 6)

$$\begin{aligned} \mathbf{a}_1 &= a(\sqrt{3}, 0) \\ \mathbf{a}_2 &= a\left(\frac{\sqrt{3}}{2}, \frac{3}{2}\right) \end{aligned}$$

and the distance vectors between nearest neighbours are

$$\begin{aligned} \boldsymbol{\delta}_1 &= \frac{a}{2}(\sqrt{3}, -1) \\ \boldsymbol{\delta}_2 &= a(0, 1) \\ \boldsymbol{\delta}_3 &= \frac{a}{2}(-\sqrt{3}, -1) \end{aligned}$$

The area of the unit cell is $\Omega_c = \frac{3\sqrt{3}}{2}a^2$. Starting from eq. 19, the graphene Hamiltonian is obtained by invoking translational invariance of the unit cell $t_{\mu\nu}(\mathbf{R}_m, \mathbf{R}_n) = t_{\mu\nu}(\mathbf{R}_m - \mathbf{R}_n)$ and

$$t_{AB}(\boldsymbol{\delta}_1) = t_{AB}(\boldsymbol{\delta}_2) = t_{AB}(\boldsymbol{\delta}_3) = -t.$$

The remaining non-zero hoppings are found by using $t_{AB} = t_{BA}$. The on-site energies $t_{AA}(\mathbf{0})$ and $t_{BB}(\mathbf{0})$ are taken to be zero. A factor of two is included due to spin degeneracy. These objects were calculated numerically

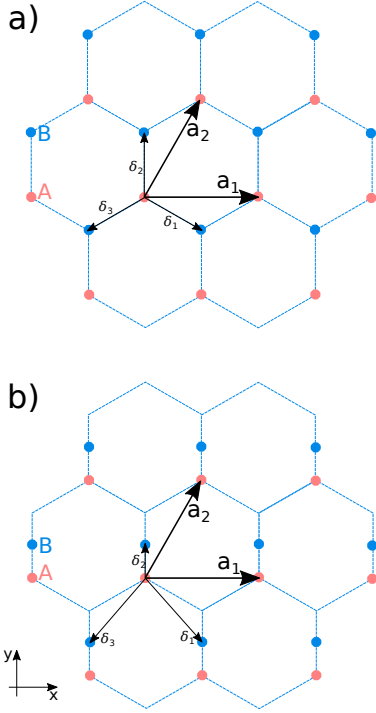


Figure 6: a) Honeycomb lattice and choice of primitive vectors. b) Honeycomb lattice with one of the sublattices displaced.

and used to obtain the first-order optical conductivity for graphene, as seen in Figure 7. We used a lattice with 4096 unit cells in each direction and 2048 Chebyshev moments in the expansion. The resulting plot is compared to the results obtained in [21] through k -space integration of a translation-invariant system.

B. Hexagonal Boron Nitride

The only difference relative to graphene is found in the on-site energies. Let $t_{AA}(\mathbf{0}) = \Delta/2$ and $t_{BB}(\mathbf{0}) = -\Delta/2$. In this model, the rank 1 and rank 3 Γ matrices are identically zero, so the second-order conductivity may be calculated resorting only to rank 2 Γ matrices. The calculation is thus simplified tremendously because the conductivity reduces to

$$\sigma^{\alpha\beta\gamma}(\omega_1, \omega_2) = \frac{ie^3}{\Omega_c \omega_1 \omega_2 \hbar^3} \times \left[\sum_{nm} \Lambda_{nm}(\omega_2) \Gamma_{nm}^{\alpha\beta,\gamma} + \frac{1}{2} \sum_{nm} \Lambda_{nm}(\omega_1 + \omega_2) \Gamma_{nm}^{\alpha,\beta\gamma} \right].$$

The indices n, m are understood to be summed over. The photoconductivity may be calculated from this formula by setting $\omega_1 = \omega = -\omega_2$ and the numerical results are shown in Figure 8. Again, we used 4096 unit cells in each lattice direction and 2048 Chebyshev moments and

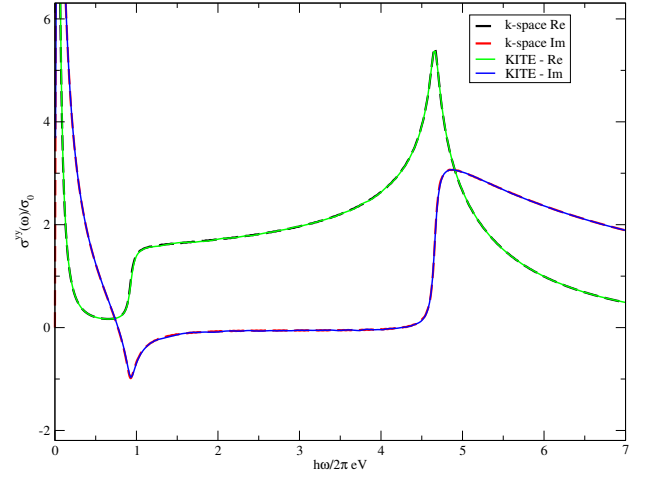


Figure 7: First-order longitudinal yy conductivity for graphene in units of $\sigma_0 = e^2/\hbar$. Hopping parameter: $t = 2.33\text{eV}$, temperature: $T = 2.33\text{mK}$, chemical potential: $\mu = 0.466\text{eV}$, broadening parameter: $\lambda = 38.8\text{meV}$, number of Chebyshev moments used: $M = 2048$, lattice size: $L = 4096 \times 4096$. The solid curves represent the optical conductivity obtained by KITE (real part in green, imaginary in blue). The superimposed dashed lines are obtained in [21].

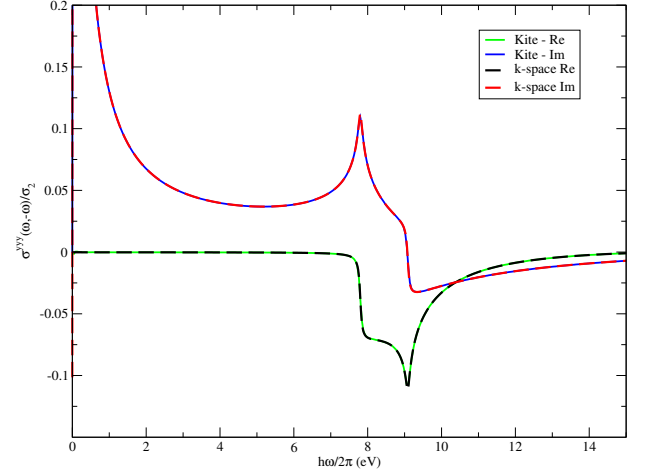


Figure 8: Second-order yyy photoconductivity for h-BN. Hopping parameter: $t = 2.33\text{eV}$, temperature: $T = 0\text{K}$, chemical potential: $\mu = 0\text{eV}$, gap $\Delta = 7.80\text{eV}$ broadening parameter: $\lambda = 39\text{meV}$, number of Chebyshev moments used: $M = 2048$, lattice size: $L = 4096 \times 4096$. The imaginary part disappears after the photoconductivity is properly symmetrized.

compare the results with the ones obtained by integrating in k -space, just like in the previous subsection. For convenience, we define the constant $\sigma_2 = e^3 a / 4t\hbar$ [9] in terms of the hopping integral t and the lattice parameter a .

To test the full formula, we must further break the symmetry. Displacing one of the sublattices relatively to each other yields nonzero rank 3 Γ matrices.

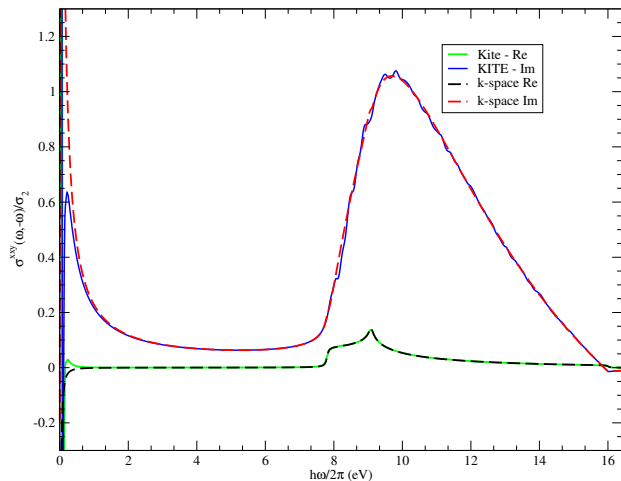


Figure 9: Second-order xy conductivity for dislocated hBN. Hopping parameter: $t = 2.33\text{eV}$, temperature: $T = 0\text{K}$, chemical potential: $\mu = 0\text{eV}$, gap $\Delta = 7.8\text{eV}$ broadening parameter: $\lambda = 39\text{meV}$, number of Chebyshev moments used: $M = 512$, lattice size: $L = 1024 \times 1024$.

C. Sublattice displacement

All the hopping parameters in this system are exactly the same as in regular hBN. The only difference is in the distance between atoms, which changes the velocity operators while keeping the Hamiltonian intact (See Figure 6).

The primitive vectors are identical, but the nearest-neighbour vectors are different:

$$\begin{aligned}\delta_1 &= a \left(\frac{\sqrt{3}}{2}, -1 \right) \\ \delta_2 &= a \left(0, \frac{1}{2} \right) \\ \delta_3 &= a \left(-\frac{\sqrt{3}}{2}, -1 \right).\end{aligned}$$

One of the sublattices was translated in the y direction by $a/2$. The second-order yyy conductivity remains zero, but now the xy photoconductivity is no longer zero and can be seen in Figure 9. The lattice size and number of polynomials used was reduced to 1024 and 512 respectively, due to the greatly increased computational cost. At lower frequencies, the results start to diverge due to the relatively low resolution.

VI. CONCLUSIONS

We developed an out-of-equilibrium expansion of the non-linear optical response of non-interacting systems using the Keldysh formalism and expressed everything

in terms of traces of operators. This provides a basis-independent expression for the linear and non-linear optical conductivities. This drops the requirement of translation invariance and allows us to include magnetic fields and disorder in our Tight-Binding calculations. We also provide a diagrammatic representation of this expansion, which makes it a very straightforward process to obtain those expressions.

The expressions for the non-linear conductivities are calculated numerically with resort to an expansion in Chebyshev polynomials and a stochastic evaluation of the trace, in close resemblance to the Kernel Polynomial Method (KPM). We provide the mapping that takes the aforementioned expressions and converts them to a numerically-suited object to be calculated with spectral methods. This is only possible because of the careful way these expressions were constructed in the first place.

We built an open-source software that is able to calculate the first- and second-order optical conductivities of very large 2D tight-binding systems (10^{10} atoms) with disorder and magnetic fields. This software is used to obtain the first- and second-order conductivities of Graphene and hexagonal Boron Nitride. These same quantities were calculated independently with the usual integration in k -space and the results are in great agreement, proving the validity of our method.

This paper serves as a proof of concept and the effects of disorder on the nonlinear optical properties of 2D materials will be explored in a future paper.

VII. ACKNOWLEDGEMENTS

The work of SMJ is supported by Fundação para a Ciência e Tecnologia (FCT) under the grant PD/BD/142798/2018. The authors acknowledge financing of Fundação da Ciência e Tecnologia, of COMPETE 2020 program in FEDER component (European Union), through projects POCI-01-0145-FEDER-02888 and UID/FIS/04650/2013. We'd also like to thank JMB Lopes dos Santos, GB Ventura, DJ Passos and D Parker for their helpful comments and suggestions regarding this paper.

-
- [1] B. Amorim. 2015. 3rd order perturbation theory: Keldysh formalism. (March 2015).
 - [2] M Bass, PA Franken, JF Ward, and G Weinreich. 1962. Optical rectification. *Physical Review Letters* 9, 11 (1962), 446.
 - [3] Francesco Bonaccorso, Zicai Sun, Tawfique Hasan, and AC Ferrari. 2010. Graphene Photonics and Optoelectronics. 4 (06 2010).
 - [4] Aires Ferreira and Eduardo R. Mucciolo. 2015. Critical Delocalization of Chiral Zero Energy Modes in Graphene.

- Phys. Rev. Lett.* 115 (Aug 2015), 106601. Issue 10. <https://doi.org/10.1103/PhysRevLett.115.106601>
- [5] RP Feynman. 1963. RP Feynman and FL Vernon, *Ann. Phys.(NY)* 24, 118 (1963). *Ann. Phys.(NY)* 24 (1963), 118.
- [6] P. A. Franken, A. E. Hill, C. W. Peters, and G. Weinreich. 1961. Generation of Optical Harmonics. *Phys. Rev. Lett.* 7 (Aug 1961), 118–119. Issue 4. <https://doi.org/10.1103/PhysRevLett.7.118>
- [7] Walter Gautschi. 1970. On the construction of Gaussian quadrature rules from modified moments. *Math. Comp.* 24, 110 (1970), 245–260.
- [8] M.M. Glazov and S.D. Ganichev. 2014. High frequency electric field induced nonlinear effects in graphene. *Physics Reports* 535, 3 (2014), 101 – 138. <https://doi.org/10.1016/j.physrep.2013.10.003> High frequency electric field induced nonlinear effects in graphene.
- [9] F Hipolito, Thomas G Pedersen, and Vitor M Pereira. 2016. Nonlinear photocurrents in two-dimensional systems based on graphene and boron nitride. *Physical Review B* 94, 4 (2016), 045434.
- [10] Radi A Jishi. 2013. *Feynman diagram techniques in condensed matter physics*. Cambridge University Press.
- [11] Leonid Veniaminovich Keldysh. 1964. Diagram technique for nonequilibrium processes. *Zh. Eksp. Teor. Fiz.* 47 (1964), 1018.
- [12] JV Lopes, SM João, A Ferreira, L Covaci, M Andelkovic, and T Rappoport. 2018. Quantum KITE. Website: <https://quantum-kite.com/>.
- [13] S A Mikhailov and K Ziegler. 2008. Nonlinear electromagnetic response of graphene: frequency multiplication and the self-consistent-field effects. *Journal of Physics: Condensed Matter* 20, 38 (2008), 384204. <http://stacks.iop.org/0953-8984/20/i=38/a=384204>
- [14] GHC New and JF Ward. 1967. Optical third-harmonic generation in gases. *Physical Review Letters* 19, 10 (1967), 556.
- [15] Daniel E Parker, Takahiro Morimoto, Joseph Orenstein, and Joel E Moore. 2018. Diagrammatic approach to nonlinear optical response with application to Weyl semimetals. *arXiv preprint arXiv:1807.09285* (2018).
- [16] DJ Passos, GB Ventura, JM Viana Parente Lopes, JMB Lopes dos Santos, and NMR Peres. 2018. Nonlinear optical responses of crystalline systems: Results from a velocity gauge analysis. *Physical Review B* 97, 23 (2018), 235446.
- [17] Rudolph Peierls. 1933. Zur theorie des diamagnetismus von leitungselektronen. *Zeitschrift für Physik* 80, 11-12 (1933), 763–791.
- [18] RA Sack and AF Donovan. 1971. An algorithm for Gaussian quadrature given modified moments. *Numer. Math.* 18, 5 (1971), 465–478.
- [19] Julian Schwinger. 1961. Brownian motion of a quantum oscillator. *J. Math. Phys.* 2, 3 (1961), 407–432.
- [20] J. E. Sipe and Ed Ghahramani. 1993. Nonlinear optical response of semiconductors in the independent-particle approximation. *Phys. Rev. B* 48 (Oct 1993), 11705–11722. Issue 16. <https://doi.org/10.1103/PhysRevB.48.11705>
- [21] G. B. Ventura, D. J. Passos, J. M. B. Lopes dos Santos, J. M. Viana Parente Lopes, and N. M. R. Peres. 2017. Gauge covariances and nonlinear optical responses. *Phys. Rev. B* 96 (Jul 2017), 035431. Issue 3. <https://doi.org/10.1103/PhysRevB.96.035431>
- [22] Alexander Weisse, Gerhard Wellein, Andreas Alvermann, and Holger Fehske. 2006. The kernel polynomial method. *Reviews of modern physics* 78, 1 (2006), 275.
- [23] Fourier convention: $f(t) = (2\pi)^{-1} \int d\omega e^{-i\omega t} \tilde{f}(\omega)$.
- [24] These matrices were explicitly calculated in the \mathbf{k} basis and shown to be exactly zero.